Available online at www.sciencedirect.com
SCIENCE DIRECT
Catalysis Today 104 (2005) 126–130
CATALYSIS TODAY
www.elsevier.com/locate/cattod

Oxygen permeation study of perovskite hollow fiber membranes

Cristina Tablet [a], Gerd Grubert [a], Haihui Wang [a,*], Thomas Schiestel [b], Michael Schroeder [c], Bernd Langanke [d], Jürgen Caro [a]

[a] University of Hanover, Institute of Physical Chemistry and Electrochemistry, Callinstr. 3-3A, D-30167 Hanover, Germany
[b] Fraunhofer Institute of Interfacial Engineering and Biotechnology (IGB), Nobelstr. 12, D-70569 Stuttgart, Germany
[c] Institute of Physical Chemistry I, RWTH Aachen, Templergraben 59, D-52056 Aachen, Germany
[d] Uhde GmbH, Friedrich-Uhde-Str. 15, D-44141 Dortmund, Germany

Available online 6 May 2005

Abstract

The first oxygen permeation data of a dense hollow fiber perovskite membrane based on $BaCo_xFe_yZr_zO_{3-\delta}$ are reported. The hollow fiber was prepared by a phase inversion process. Dense fibers were obtained with the following typical geometries: outer diameter, 800–900 μm; inner diameter, 500–600 μm; length, 30 cm. The O_2-permeation through the hollow fiber perovskite membrane was studied in a high-temperature gas permeation cell under different operation conditions. The increase of the helium gas flow rate reduces the oxygen partial pressure (p_{O_2}) on the core side and a higher oxygen permeation flux is observed. High oxygen flux of 0.73 m^3 (O_2)/(m^2 (membrane) h) was achieved at 850 °C under the operation parameters F_{air} (shell side) = 150 ml/min and F_{He} (core side) = 30 ml/min. The oxygen partial pressure dependence of the O_2 permeation flux indicated an interplay of both surface reaction and bulk diffusion as rate limiting steps. During 5 days of permeation a high and stable oxygen flux was observed. X-ray diffraction patterns of fresh and spent membranes after the permeation measurements revealed that no degradation after oxygen permeation appears.

Keywords: Perovskite; Membrane; POM; Syngas; Oxygen separation; Hollow fiber

1. Introduction

Mixed-conducting oxides with high electron and oxygen ion conductivities (MIEC) are applied as ceramic membranes to separate oxygen from other gases by selective permeation [1–3]. The very high O_2 separation factor is achieved by oxygen ion transport through the dense membrane at temperatures generally higher than 700 °C. The driving force is the oxygen partial pressure gradient over the membrane. At the high oxygen partial pressure side, the oxygen molecules adsorb on the membrane surface, dissociate into atoms which become ionized and migrate through the membrane to the low oxygen partial pressure side of the membrane. Finally, they release electrons forming oxygen atoms and molecules by recombination. In the opposite direction, the electrons move through the membrane thus ensuring local electrical neutrality.

Perovskite-type oxides are well known and well examined candidates for MIEC-membranes. These materials have not only been studied for simple oxygen separation, but also for delivering oxygen for partial oxidation of methane to synthesis gas (POM) in membrane reactors [4–6]. Therefore, in addition to high oxygen ion and electron mobility a sufficient chemical and mechanical stability at elevated operating temperatures is needed for industrial applications. It is also very important that these materials need a high structural stability towards the reducing atmosphere on the reaction side because of the very low oxygen partial pressures ($<10^{-15}$ mbar) on the synthesis gas side of the membrane.

Generally, disk-shaped membranes were used to construct membrane reactors for the POM reaction since they can be easily prepared using conventional synthesis routes [7–9]. However, this membrane geometry does not meet the requirements for an industrial application because of the low effective area of the disks and the difficult assembling to a reactor module [10]. Tubular shaped membranes have

* Corresponding author. Tel.: +49 511 762 3080; fax: +49 511 762 19121.
E-mail address: Haihui.Wang@pci.uni-hannover.de (H. Wang).

0920-5861/$ – see front matter © 2005 Elsevier B.V. All rights reserved.
doi:10.1016/j.cattod.2005.03.064

already been reported in the literature [11,12]. From modeling studies of different tubular shaped membranes, it was found that the hollow fiber geometry can provide the highest oxygen permeation flux (J_{O_2}) as well as the largest membrane area per unit packing volume when assembled to a membrane reactor [10].

In this paper, the first oxygen permeation data of a hollow fiber perovskite membrane are reported. This work is focused on the effect of different temperatures (650–850 °C), of various air (F_{air} = 20–150 ml/min) and sweep gas (F_{He} = 10–100 ml/min; F_{Ne} = 0.46 ml/min) flows as well as the influence of different partial pressures on the oxygen permeation flux. Furthermore, we attempted to understand the limiting step of oxygen permeation through hollow fiber perovskite membranes.

2. Experimental

Dense hollow fiber perovskite membranes were manufactured at the Fraunhofer Institute for Interfacial Engineering and Biotechnology (IGB) by a phase inversion process. The perovskite powder $BaCo_xFe_yZr_zO_{3-\delta}$ was dispersed in a polymer solution and the slurry was spun through a spinneret. After sintering, the geometry of the fibers was as follows: outer diameter = 800–900 μm; inner diameter = 500–600 μm; length = 30 cm.

The phase structure of the hollow fiber perovskite membrane after sintering and after O_2-permeation experiment was characterized by X-ray diffraction (PHILIPS-PW1710, Cu Kα radiation) from 20° to 90° with a step width of 0.05°. Micrographs of the hollow fiber perovskite membrane were obtained with a scanning electron microscope (Jeol-JSM-6700F).

The O_2-permeation of the hollow fiber perovskite membrane was tested in a high-temperature gas permeation cell at (i) different temperatures between 650 and 850 °C, (ii) different flow rates of air and sweep gas as well as (iii) different O_2-partial pressures. At the shell side air or synthetic air of different ratios of nitrogen and oxygen were used as the feed with flow rates from 20 to 150 ml/min. Pure He (99.995%) and Ne (>99.995%) as an internal standard (constant F = 0.46 ml/min) flowed on the core side of the membrane at a flow rate varying from 10 to 100 ml/min. The inlet gas flow rates were controlled by mass flow controllers (Bronkhorst). The hollow fiber perovskite membrane was cold-sealed with high-temperature silicon seals at the ends, which were outside the hot zone of the oven. The gases were pre-heated to 180 °C before they were fed to the permeator and all gas lines to the gas chromatograph were heated to 180 °C. The gases at the exit of the permeator were analyzed by a gas chromatograph (GC-Agilent 6890) equipped with the Carboxen 1000 column (Supelco). The oxygen permeation flux J_{O_2} (ml/cm^2 min) was calculated from the total flow rate F (ml/min), the oxygen concentration of the exit gas C_{O_2} (%), and the effective area of the membrane tube S (cm^2) based on the following equation:

$$J_{O_2} = \frac{F \times C_{O_2}}{S}$$

The concentration of the permeated O_2 was determined by calibration. The total flow rate of the components in the effluent gas was calculated from the change of the Ne concentration before and after the permeator. If air leaked through the seals, the corresponding amount of O_2 was subtracted based on the N_2 signal when the O_2 permeation flux was calculated. Leakage of O_2 due to the imperfect sealing at high temperature was less than 0.3% for all samples. The experimental setup for the oxygen permeation measurements of dense hollow fiber perovskite membranes is shown in Fig. 1.

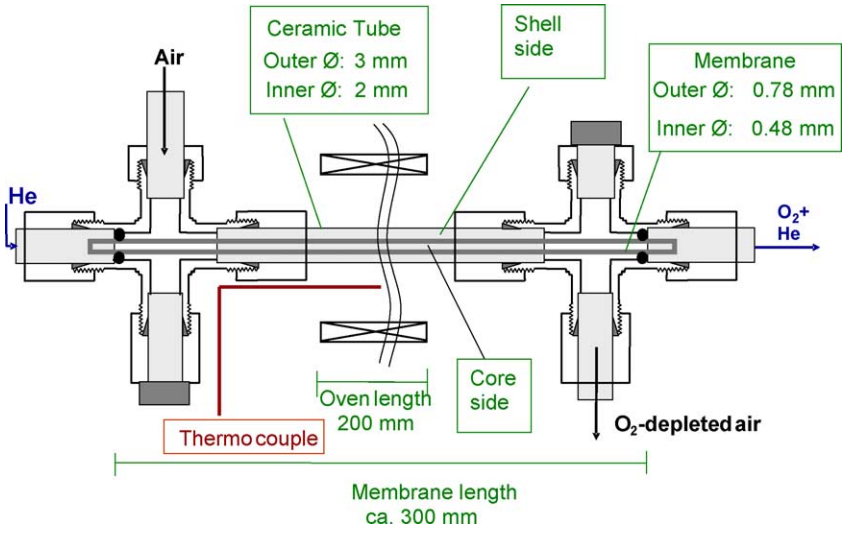

Fig. 1. Schematic diagram of the high temperature oxygen permeation cell for testing a dense hollow fiber perovskite membrane.

3. Results and discussion

Fig. 2 shows the micrograph of a fresh hollow fiber perovskite membrane sintered at 1300 °C for 6 h. From this picture, we can see that the membrane is dense and no open holes can be found in the bulk of the membrane although a large amount of organic additives (about 45 wt.%) is used during the spinning process. When the hollow fiber was arranged in the permeation cell as shown in Fig. 1, at room temperature no nitrogen was found by analysis of the gases from the core side when nitrogen was fed to the shell side and helium was fed to the core side. This also proves that the hollow fiber perovskite membrane is gas tight.

Fig. 3 shows the variation of the air flow rate between 20 and 150 ml/min at 850 °C, while the helium flow rate as the sweep on the core side was kept at 30 ml/min. It was found that the oxygen permeation flux increased with increasing air flow rate until the air flow rate was higher than 80 ml/min. Further increase of the air flow rate did not lead to a further increase of the oxygen flux. These results indicate that air should be sufficiently delivered to use the separation capacity of the hollow fiber perovskite membrane properly. It can be concluded that for air flow rates higher than 80 ml/min a further increase of the air flow would not change the shell side concentration profile, being already flat at the level of the inlet concentration. In order to eliminate the effect of the air flow rate on the oxygen permeation flux, we chose a constant air flow rate of 150 ml/min in the subsequent studies.

The dependence of the oxygen permeation flux of the hollow fiber perovskite membrane on the He flow rates on the core side at 850 °C is shown in Fig. 4. During this experiment, the He flow rate was varied from 10 to 100 ml/min and the air flow rate was kept constant at 150 ml/min. As observed for the variation of the air flow rate, the oxygen permeation flux was found to increase with increasing helium flow rate. However, no saturation of the oxygen

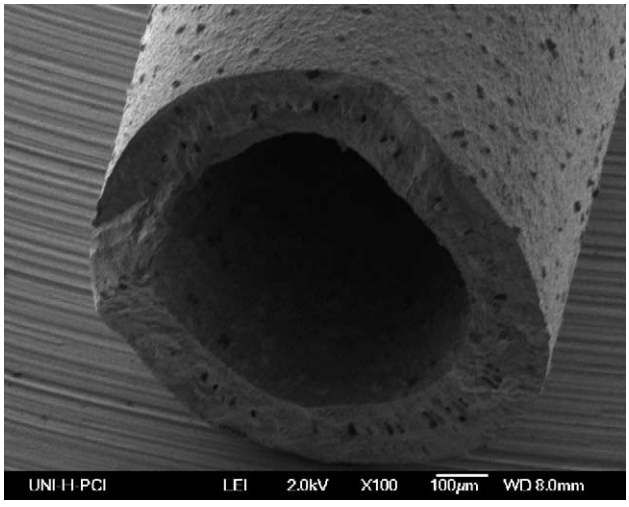

Fig. 2. Cross-section of the fresh perovskite hollow fiber membrane after sintering at 1300 °C for 6 h in air.

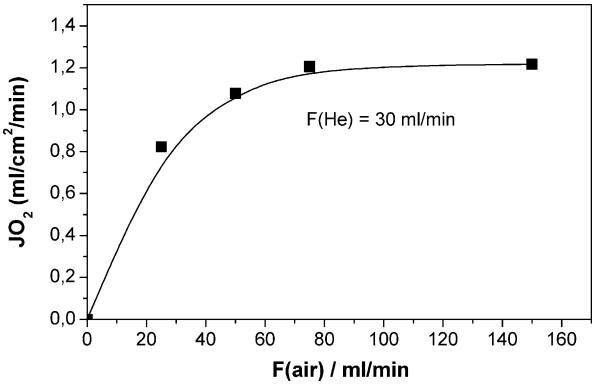

Fig. 3. Oxygen permeation flux through the dense hollow fiber perovskite membrane as a function of the air flow rate. Permeation conditions: F_{air} (shell side) = 20–150 ml/min; F_{He} (core side) = 30 ml/min; T = 850 °C; $p'_{total} = p''_{total}$ = 1.2 bar.

permeation flux was observed when the helium flow rate increased from 10 to 100 ml/min because the increase of the helium flow rate reduces the oxygen partial pressure (p''_{O_2}) on the core side, and thus a higher oxygen permeation flux is obtained.

The temperature dependence of the oxygen permeation flux was studied between 650 and 850 °C. The flow rates of air and He were 150 and 30 ml/min, respectively. Fig. 5 shows the increase of the oxygen permeation flux with increasing temperature attributed to the promotion of the oxygen diffusion and the oxygen surface reaction rates. In the corresponding Arrhenius plot (Fig. 6) a straight line is found which gives an apparent activation energy of 133 kJ/mol for the hollow fiber perovskite membrane. Further research indicated that the rate limiting step of the disk-type membrane with 1 mm thickness is bulk diffusion. It was necessary, therefore, to study the limiting step of the oxygen permeation through the hollow fiber perovskite membrane as it will be shown in the next part of this paper.

The dependence of the oxygen permeation flux on the oxygen partial pressure gradient and the membrane wall

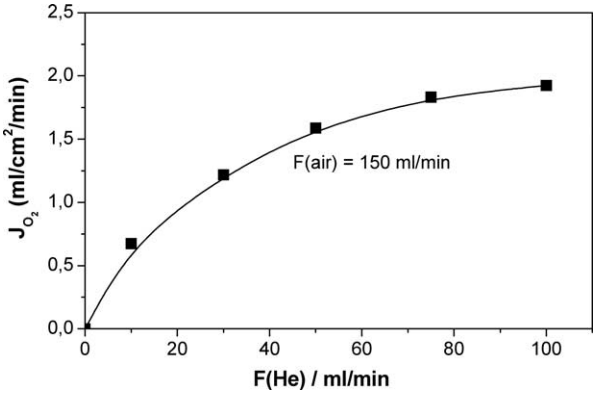

Fig. 4. Oxygen permeation flux through the dense hollow fiber perovskite membrane as a function of the helium flow rate. Permeation conditions: F_{air} (shell side) = 150 ml/min; F_{He} (core side) = 10–100 ml/min; T = 850 °C; $p'_{total} = p''_{total}$ = 1.2 bar.

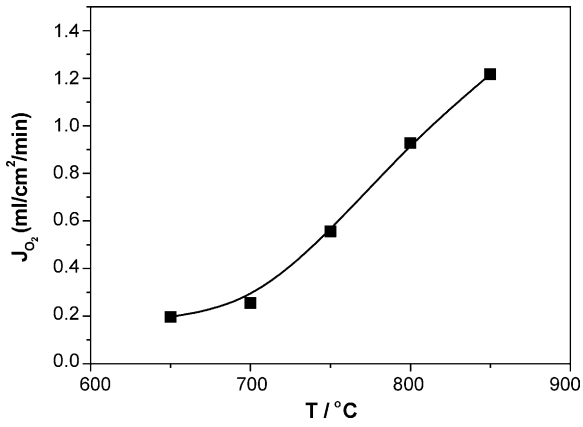

Fig. 5. Oxygen permeation flux through the dense hollow fiber perovskite membrane as a function of temperature. Permeation conditions: F_{air} (shell side) = 150 ml/min; F_{He} (core side) = 30 ml/min; T = 650–850 °C.

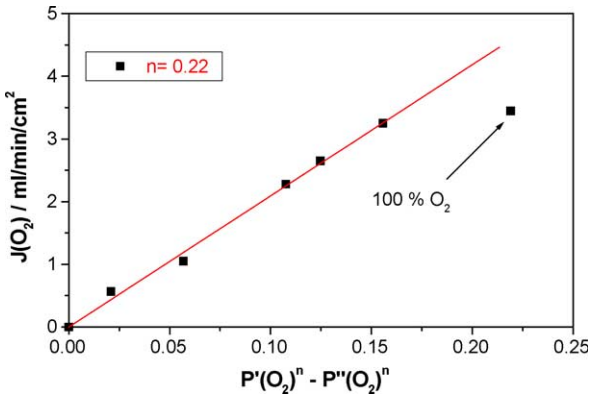

Fig. 7. Linearised plot of the Wagner equation: J(O_2) as a function of the oxygen partial pressure gradient for dense hollow fiber perovskite membrane. Permeation conditions: $F_{(O_2+N_2)}$ (shell side) = 150 ml/min; F_{He} (core side) = 30 ml/min; p'_{O_2} = 0.12–1.2 bar; T = 850 °C; $p'_{total} = p''_{total}$ = 1.2 bar.

thickness is an effective way to estimate the rate determining step. This dependence is well described by the Wagner Theory [13]:

$$J_{O_2} \approx -\frac{\delta^0 D_v}{4V_m nL}((p''_{O_2})^n - (p'_{O_2})^n) \quad (1)$$

where δ^0 is the number of oxygen defects at p_{O_2} = 1 bar ($\delta = \delta^0 \times p_{(O_2)^n}$), D_v the vacancy diffusion coefficient ($D_v = D_v^0 e^{E_D/RT}$), E_D the activation energy of diffusion, V_m the molar volume of perovskite, L the wall thickness of the membrane and n is the fit parameter. From the value of n the rate limiting process can be identified. Generally, for values of $n > 0.5$ the oxygen permeation is predominantly governed by the reaction of oxygen with the membrane surface. For negative values of n the oxygen permeation is dominated by the oxygen ion diffusion through the membrane [14].

The oxygen permeation properties of the hollow fiber perovskite membranes were studied with different oxygen partial pressures on the shell side (p'_{O_2}) and on the core side (p''_{O_2}) at 850 °C. The total flow rate of the O_2/N_2 mixture on the shell side was 150 ml/min and different oxygen partial pressure (p'_{O_2}) on the shell side were obtained by adjusting the ratio of N_2 and O_2. The helium flow rate on the core side was kept constant at 30 ml/min. The oxygen permeation flux increased with increasing oxygen partial pressure on the shell side due to the increase of the oxygen gradient across the membrane. This result indicates that a high oxygen permeation flux for industrial applications can be achieved by increasing the air pressure on the shell side. In order to understand the limiting step of the oxygen permeation through the hollow fiber perovskite membrane, we fitted our data with Eq. (1). Fig. 7 gives the best linear fit for J_{O_2} as a function of the oxygen partial pressure gradient for n = 0.22, which suggests that the permeation process is partly controlled by the oxygen surface exchange kinetics.

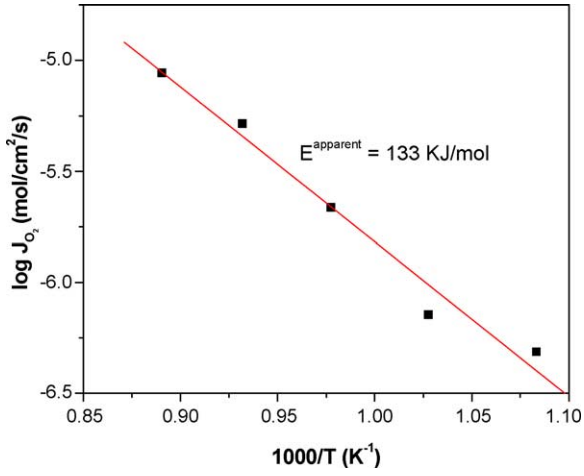

Fig. 6. Arrhenius plot of the oxygen permeation flux of the dense hollow fiber perovskite membrane. Permeation conditions: F_{air} (shell side) = 150 ml/min; F_{He} (core side) = 30 ml/min; T = 650–850 °C.

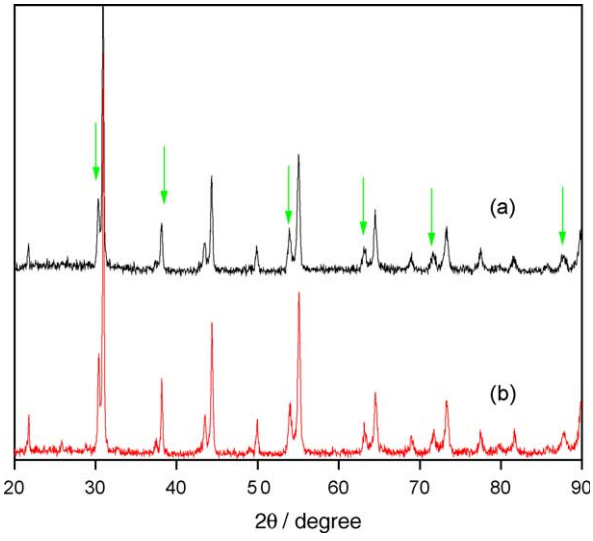

Fig. 8. XRD patterns of the fresh and spent perovskite hollow fiber membranes. (a) Fresh membrane and (b) membrane after oxygen permeation for 5 days between 650 and 850 °C.

Table 1
Comparison of the oxygen permeation data for different geometries of perovskite membranes: hollow fiber and disk membranes

	Hollow fiber	Disk
F_{air} (ml/min)	150 (shell side)	150
F_{He} (ml/min)	30 (core side)	30
T (°C)	850	850
Membrane surface (cm^2)	4.08	1.00
Membrane thickness (mm)	0.16	1
J_{O_2} (ml/(min cm^2))	1.05	0.30
$J_{(N_2)^{defect}}/J_{O_2}$	0.003	–

Phase stability is very important for an industrial perovskite application. XRD was used to characterize the perovskite structure of the membrane before and after operation. The XRD patterns of the perovskite membrane after sintering for 6 h at 1300 °C in air and after oxygen permeation for 5 days at temperatures between 650 and 850 °C are shown in Fig. 8. In the fresh membrane, in addition to the cubic perovskite structure an unidentified by-phase was found. The concentration of this by-phase was unchanged after 5 days of operation. In contrast, the starting perovskite powder for spinning showed a pure perovskite structure. It is supposed, therefore, that this by-phase is formed during sintering. However, no difference between the fresh and spent membrane was observed. Thus, X-ray analysis of the material before and after the experiment confirmed that the material is phase stable.

For comparison, a disk-type membrane of the same perovskite composition was prepared and the oxygen permeation was tested under the same conditions. Table 1 shows the O_2-permeation data for hollow fiber and disk geometries. In comparison to the disk-shaped membrane a lower F_{air} saturation flow rate was obtained for the hollow fiber perovskite membrane. Higher oxygen fluxes for the hollow fiber geometry were detected in comparison with the disk membrane.

4. Conclusions

Dense hollow fiber perovskite membranes of the composition $BaCo_xFe_yZr_zO_{3-\delta}$ were prepared by a phase inversion process. After sintering, fibers with an outer diameter of 800–900 μm, an inner diameter of 500–600 μm and a length of 30 cm were obtained. From an XRD phase study it was found that the dense hollow fiber membrane after sintering at 1300 °C was not a pure perovskite. The O_2-permeation rate was stable at 850 °C during 5 days, which confirms the stable phase structure of the hollow fiber membranes. No signs of degradation of the perovskite material after O_2-permeation measurements were observed by X-ray diffraction. A high oxygen flux of 0.63 m^3 (O_2)/(m^2 (membrane) h) was achieved at 850 °C when F_{air} (shell side) = 150 ml/min and F_{He} (core side) = 30 ml/min. From the temperature as well as the oxygen gradient dependence of J_{O_2} it follows that both surface reaction and bulk-diffusion are the rate-determining steps for the oxygen flux. The high oxygen flux renders the hollow fiber geometry for MIEC membranes as a possible candidate for industrial POM reactors.

Acknowledgements

The authors gratefully acknowledge the financial support of the BMBF for project 03C0343A under the auspices of ConNeCat. H. Wang greatly thanks the financial support from the Alexander von Humboldt Foundation.

References

[1] U. Balachandran, J.T. Dusek, R.L. Mieville, R.B. Poeppel, M.S. Kleefisch, S. Pei, T.P. Kobylinski, C.A. Udovich, A.C. Bose, Appl. Catal. A Gen. 133 (1995) 19.
[2] S. Kim, Y.L. Yang, A.J. Jacobson, B. Abeles, Solid State Ionics 106 (1998) 189.
[3] S. Diethelm, J.V. Herle, J. Eur. Ceram. Soc. 24 (2004) 1319.
[4] H. Dong, Z.P. Shao, G.X. Xiong, J.H. Tong, S.S. Sheng, W.S. Yang, Catal. Today 67 (2001) 3.
[5] V.A. Tsipouriari, Z. Zhang, X.E. Verykios, J. Catal. 179 (1998) 283.
[6] H.H. Wang, Y. Cong, W.S. Yang, Catal. Today 82 (2003) 157.
[7] J.H. Tong, W.S. Yang, R. Cai, B. Zhu, L. Lin, Catal. Lett. 78 (2002) 129.
[8] Z.P. Shao, G.X. Xiong, Y. Cong, H. Dong, J.H. Tong, W.S. Yang, J. Membr. Sci. 172 (2000) 177.
[9] H. Dong, Z. Shao, G. Xiong, J. Tong, S. Sheng, W. Yang, Catal. Today 67 (2001) 3.
[10] H.H. Wang, R. Wang, D.T. Liang, W.S. Yang, J. Membr. Sci. 243 (2004) 405.
[11] H.H. Wang, Y. Cong, W.S. Yang, J. Membr. Sci. 210 (2002) 259.
[12] D.C. Zhu, X.Y. Xu, S.J. Feng, W. Liu, C.S. Chen, Catal. Today 82 (2003) 151.
[13] C. Wagner, W. Schottky, Z. Phys. Chem. B 11 (1930) 25.
[14] K.Q. Huang, M. Schroeder, J.B. Goodenough, in: Proceedings of the International Symposium on Solid State Ionic Devices, The Electrochemical Society Proceedings Series, Pennington, NY, PV 99-13, 1999, p. 95.